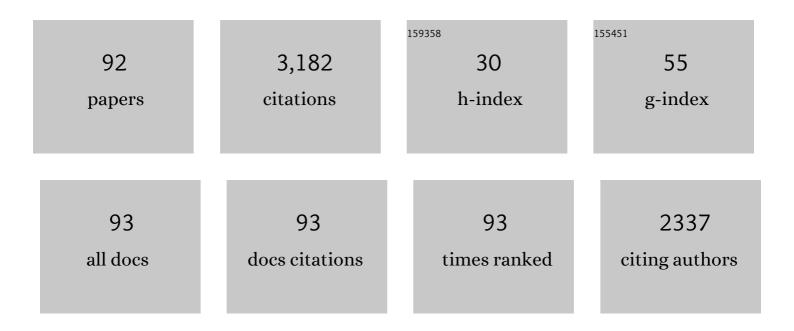


List of Publications by Year in descending order

Source: https://exaly.com/author-pdf/5719274/publications.pdf Version: 2024-02-01



IF # ARTICLE CITATIONS Efficient and Durable Cu₃PFeP for Hydrogen Evolution from Seawater with Current Density Exceeding 1 A cm^{â€"2}. ACS Ápplied Energy Materials, 2022, 5, 2909-2917. Demonstration of a New Characterization Method for Weak Measurement. Frontiers in Chemistry, 9 1.8 0 2022, 10, . ZIF-derived holey electrode with enhanced mass transfer and N-rich catalytic sites for high-power and 7.1 long-life vanadium flow batteries. Journal of Energy Chemistry, 2022, 72, 545-553. Specific detection of glucose by an optical weak measurement sensor. Biomedical Optics Express, 2021, 4 1.5 3 12, 5128. In situ detection of electrochemical reaction by weak measurement. Optics Express, 2021, 29, 19292. 1.7 Optimization of the Weak Measurement System by Determining the Optimal Total Phase Difference. IEEE 1.0 0 6 Photonics Journal, 2021, 13, 1-8. High-Throughput Chiral Molecule Determination Based on Multi-Channel Weak Measurement. IEEE 1.0 Photonics Journal, 2021, 13, 1-12. Imaging Sensor for the Detection of the Flow Battery Via Weak Value Amplification. Analytical 8 3.2 7 Chemistry, 2021, 93, 12914-12920. Tailoring the vanadium/proton ratio of electrolytes to boost efficiency and stability of vanadium 5.1 54 flow batteries over a wide temperature range. Applied Energy, 2021, 301, 117454. MoS2â€"CoS2 heteronanosheet arrays coated on porous carbon microtube textile for overall water 10 4.0 32 splitting. Journal of Power Sources, 2021, 514, 230580. Temperature-Insensitive Label-Free Sensors for Human IgG Based on S-Tapered Optical Fiber Sensors. IEEE Access, 2021, 9, 116286-116293. Characterizing the Onset Potential Distribution of Pt/C Catalyst Deposition by a Total Internal 12 5.2 6 Reflection Imaging Method. Small, 2021, 17, e2102407. An Optimized Angular Total Internal Reflection Sensor With High Resolution in Vanadium Flow 2.4 Batteries. IEEE Transactions on Instrumentation and Measurement, 2020, 69, 3170-3178. Boosting the thermal stability of electrolytes in vanadium redox flow batteries via 14 1.5 9 1-hydroxyethane-1,1-diphosphonic acid. journal of Applied Electrochemistry, 2020, 50, 255-264. Method of Reflow and Online Electrolysis in the Vanadium Redox Battery: Benefits and Limitations. 3.2 ACS Sustainable Chemistry and Engineering, 2020, 8, 10275-10283. A Waveguide-Coupled Surface Plasmon Resonance Sensor Using an Au-MgF2-Au Structure. Plasmonics, 16 1.8 12 2019, 14, 187-195. The indefinite cycle life via a method of mixing and online electrolysis for vanadium redox flow 4.0 batteries. Journal of Power Sources, 2019, 438, 226990. Revealing sulfuric acid concentration impact on comprehensive performance of vanadium 18 2.6 30

electrolytes and flow batteries. Electrochimica Acta, 2019, 303, 21-31.

Le Liu

#	Article	IF	CITATIONS
19	In situ mapping of activity distribution and oxygen evolution reaction in vanadium flow batteries. Nature Communications, 2019, 10, 5286.	5.8	45
20	Exceptional Performance of Hierarchical Ni–Fe (hydr)oxide@NiCu Electrocatalysts for Water Splitting. Advanced Materials, 2019, 31, e1806769.	11.1	124
21	Optimization of angle-pixel resolution for angular plasmonic biosensors. Sensors and Actuators B: Chemical, 2019, 283, 188-197.	4.0	17
22	Broad temperature adaptability of vanadium redox flow battery–part 4: Unraveling wide temperature promotion mechanism of bismuth for V2+/V3+ couple. Journal of Energy Chemistry, 2018, 27, 1333-1340.	7.1	41
23	Broad temperature adaptability of vanadium redox flow battery-Part 3: The effects of total vanadium concentration and sulfuric acid concentration. Electrochimica Acta, 2018, 259, 11-19.	2.6	56
24	Holey-engineered electrodes for advanced vanadium flow batteries. Nano Energy, 2018, 43, 55-62.	8.2	127
25	Real-Time Study of the Disequilibrium Transfer in Vanadium Flow Batteries at Different States of Charge via Refractive Index Detection. Journal of Physical Chemistry C, 2018, 122, 28550-28555.	1.5	15
26	Composite layer based plasmon waveguide resonance for label-free biosensing with high figure of merit. Sensors and Actuators B: Chemical, 2018, 272, 69-78.	4.0	17
27	Bifunctional effects of halloysite nanotubes in vanadium flow battery membrane. Journal of Membrane Science, 2018, 564, 237-246.	4.1	31
28	A low-cost average valence detector for mixed electrolytes in vanadium flow batteries. RSC Advances, 2018, 8, 20773-20780.	1.7	7
29	Rice Paper Reinforced Sulfonated Poly(ether ether ketone) as Low-Cost Membrane for Vanadium Flow Batteries. ACS Sustainable Chemistry and Engineering, 2017, 5, 2437-2444.	3.2	39
30	Electrochemical evaluation methods of vanadium flow battery electrodes. Physical Chemistry Chemical Physics, 2017, 19, 14708-14717.	1.3	43
31	Reduction of capacity decay in vanadium flow batteries by an electrolyte-reflow method. Journal of Power Sources, 2017, 338, 17-25.	4.0	73
32	Carbon dots promoted vanadium flow batteries for all-climate energy storage. Chemical Communications, 2017, 53, 7565-7568.	2.2	46
33	Rational use and reuse of Nafion 212 membrane in vanadium flow batteries. RSC Advances, 2017, 7, 19425-19433.	1.7	35
34	Asymmetric vanadium flow batteries: long lifespan via an anolyte overhang strategy. Physical Chemistry Chemical Physics, 2017, 19, 29195-29203.	1.3	21
35	Rapid detection of the positive side reactions in vanadium flow batteries. Applied Energy, 2017, 185, 452-462.	5.1	23
36	Membrane evaluation for vanadium flow batteries in a temperature range of â^20–50 °C. Journal of Membrane Science, 2017, 522, 45-55.	4.1	90

LE LIU

#	Article	IF	CITATIONS
37	The benefits and limitations of electrolyte mixing in vanadium flow batteries. Applied Energy, 2017, 204, 373-381.	5.1	76
38	Temperature-Regulated Surface Plasmon Resonance Imaging System for Bioaffinity Sensing. Plasmonics, 2016, 11, 771-779.	1.8	14
39	Insights into the Impact of the Nafion Membrane Pretreatment Process on Vanadium Flow Battery Performance. ACS Applied Materials & Interfaces, 2016, 8, 12228-12238.	4.0	166
40	The detection method for small molecules coupled with a molecularly imprinted polymer/quantum dot chip using a home-built optical system. Analytical and Bioanalytical Chemistry, 2016, 408, 5261-5268.	1.9	10
41	A fiber-based fluorometric system for in situ algal classification. Optics and Laser Technology, 2016, 76, 121-126.	2.2	0
42	Broad temperature adaptability of vanadium redox flow battery—Part 1: Electrolyte research. Electrochimica Acta, 2016, 187, 525-534.	2.6	127
43	Resolution enhancement of surface plasmon resonance sensors with spectral interrogation: resonant wavelength considerations. Applied Optics, 2016, 55, 884.	2.1	17
44	Broad temperature adaptability of vanadium redox flow battery—Part 2: Cell research. Electrochimica Acta, 2016, 191, 695-704.	2.6	84
45	Quantum-dots-encoded-microbeads based molecularly imprinted polymer. Biosensors and Bioelectronics, 2016, 77, 886-893.	5.3	48
46	Study on Trace Sample of Chronic Skin Ulcer with a Symmetrical Optical Waveguide-Based Surface Plasmon Resonance Biosensor. Plasmonics, 2015, 10, 1631-1637.	1.8	5
47	Self-Referenced Plasmon Waveguide Resonance Sensor Using Different Waveguide Modes. Journal of Sensors, 2015, 2015, 1-10.	0.6	9
48	An on-line spectroscopic monitoring system for the electrolytes in vanadium redox flow batteries. RSC Advances, 2015, 5, 100235-100243.	1.7	34
49	A saccharides sensor developed by symmetrical optical waveguide-based surface plasmon resonance. Journal of Innovative Optical Health Sciences, 2015, 08, 1550003.	0.5	1
50	Study on the Despeckle Methods in Angular Surface Plasmon Resonance Imaging Sensors. Plasmonics, 2015, 10, 729-737.	1.8	7
51	Noninvasive and Real-Time Plasmon Waveguide Resonance Thermometry. Sensors, 2015, 15, 8481-8498.	2.1	6
52	Decoding of Quantum Dots Encoded Microbeads Using a Hyperspectral Fluorescence Imaging Method. Analytical Chemistry, 2015, 87, 5286-5293.	3.2	25
53	Effect of degree of sulfonation and casting solvent on sulfonated poly(ether ether ketone) membrane for vanadium redox flow battery. Journal of Power Sources, 2015, 285, 195-204.	4.0	167
54	One-dimensional angular surface plasmon resonance imaging based array thermometer. Sensors and Actuators B: Chemical, 2015, 207, 254-261.	4.0	14

Le Liu

#	Article	IF	CITATIONS
55	A BIOSENSOR USING COUPLED PLASMON WAVEGUIDE RESONANCE COMBINED WITH HYPERSPECTRAL FLUORESCENCE ANALYSIS. Journal of Innovative Optical Health Sciences, 2014, 07, 1450017.	0.5	1
56	Plasmon waveguide resonance sensor using an Au–MgF ₂ structure. Applied Optics, 2014, 53, 6344.	0.9	23
57	Non-scan and real-time multichannel angular surface plasmon resonance imaging method. Applied Optics, 2014, 53, 6037.	0.9	12
58	Sulfonated Poly(Ether Ether Ketone)/Graphene composite membrane for vanadium redox flow battery. Electrochimica Acta, 2014, 132, 200-207.	2.6	120
59	CeO ₂ decorated graphite felt as a high-performance electrode for vanadium redox flow batteries. RSC Advances, 2014, 4, 61912-61918.	1.7	128
60	Properties Investigation of Sulfonated Poly(ether ether ketone)/Polyacrylonitrile Acid–Base Blend Membrane for Vanadium Redox Flow Battery Application. ACS Applied Materials & Interfaces, 2014, 6, 18885-18893.	4.0	162
61	Characterization of sulfonated poly(ether ether ketone)/poly(vinylidene) Tj ETQq1 1 0.784314 rgBT /Overlock 1 Journal of Power Sources, 2014, 272, 427-435.	0 Tf 50 507 4.0	7 Td (fluoride 63
62	An amplitude modulation fluorometric method for phytoplankton classified measure. Optik, 2014, 125, 2661-2664.	1.4	5
63	Detect the Hybridization of Single-Stranded DNA by Parallel Scan Spectral Surface Plasmon Resonance Imaging. Plasmonics, 2013, 8, 1185-1191.	1.8	14
64	Preparation and characterization of sulfonated poly(ether ether ketone)/poly(vinylidene fluoride) blend membrane for vanadium redox flow battery application. Journal of Power Sources, 2013, 237, 132-140.	4.0	94
65	Electrochemical activation of graphite felt electrode for VO2+/VO2+ redox couple application. Electrochimica Acta, 2013, 89, 429-435.	2.6	300
66	A symmetrical optical waveguide based surface plasmon resonance biosensing system. Sensors and Actuators B: Chemical, 2013, 185, 91-96.	4.0	47
67	MgF2–Au–MgF2-polydopamine based surface plasmon resonance sensor and its application in biomedical systems. Analytical Methods, 2013, 5, 6306.	1.3	6
68	Multi-Channel Hyperspectral Fluorescence Detection Excited by Coupled Plasmon-Waveguide Resonance. Sensors, 2013, 13, 13892-13902.	2.1	5
69	Online Spectroscopic Study on the Positive and the Negative Electrolytes in Vanadium Redox Flow Batteries. Journal of Spectroscopy, 2013, 2013, 1-8.	0.6	11
70	Line-scanning Raman imaging spectroscopy for detection of fingerprints. Applied Optics, 2012, 51, 3701.	0.9	17
71	Polarization-interferometry-based wavelength-interrogation surface plasmon resonance imager for analysis of microarrays. Journal of Biomedical Optics, 2012, 17, 036002.	1.4	5
72	State of charge monitoring for vanadium redox flow batteries by the transmission spectra of V(IV)/V(V) electrolytes. Journal of Applied Electrochemistry, 2012, 42, 1025-1031.	1.5	55

Le Liu

#	Article	IF	CITATIONS
73	Polarization interference interrogation of angular surface plasmon resonance sensors with wide metal film thickness tolerance. Sensors and Actuators B: Chemical, 2012, 173, 218-224.	4.0	10
74	Parallel scan hyperspectral fluorescence imaging system and biomedical application for microarrays. Journal of Physics: Conference Series, 2011, 277, 012023.	0.3	3
75	Parallel-scan based microarray imager capable of simultaneous surface plasmon resonance and hyperspectral fluorescence imaging. Biosensors and Bioelectronics, 2011, 30, 180-187.	5.3	10
76	A two-dimensional polarization interferometry based parallel scan angular surface plasmon resonance biosensor. Review of Scientific Instruments, 2011, 82, 023109.	0.6	33
77	Line-Monitoring, Hyperspectral Fluorescence Setup for Simultaneous Multi-Analyte Biosensing . Sensors, 2011, 11, 10038-10047.	2.1	5
78	Two-channel, quasi-confocal parallel scan fluorescence imaging for detection of biochips. Optics and Lasers in Engineering, 2010, 48, 849-855.	2.0	7
79	MiRNAâ€26b regulates the expression of cyclooxygenaseâ€2 in desferrioxamineâ€treated CNE cells. FEBS Letters, 2010, 584, 961-967.	1.3	56
80	Detection of methane by a surface plasmon resonance sensor based on polarization interferometry and angle modulation. Optics and Lasers in Engineering, 2010, 48, 1182-1185.	2.0	6
81	Quasi-Confocal, Multichannel Parallel Scan Hyperspectral Fluorescence Imaging Method Optimized for Analysis of Multicolor Microarrays. Analytical Chemistry, 2010, 82, 7752-7757.	3.2	19
82	An Efficient Parallel PathStack Algorithm for Processing XML Twig Queries on Multi-core Systems. Lecture Notes in Computer Science, 2010, , 277-291.	1.0	9
83	Experimental study of the optimal metal film for surface plasmon resonance. , 2009, , .		2
84	Experimental study on the influence of the metal film thickness on surface plasmon resonance biosensors. Proceedings of SPIE, 2009, , .	0.8	2
85	Study on conditions of DNA immobilization by surface plasmon resonance imaging. Proceedings of SPIE, 2009, , .	0.8	0
86	A comparison study of microarrays by fluorescence imaging and surface plasmon resonance imaging. Proceedings of SPIE, 2009, , .	0.8	0
87	A new parallel scan spectral SPR 2D sensing system. Proceedings of SPIE, 2009, , .	0.8	0
88	Immobilization of human papillomavirus DNA probe for surface plasmon resonance imaging. Proceedings of SPIE, 2009, , .	0.8	0
89	Parallel scan spectral surface plasmon resonance imaging. Applied Optics, 2008, 47, 5616.	2.1	36
90	Parallel Structural Join Algorithm on Shared-Memory Multi-Core Systems. , 2008, , .		12

Le	Τı	11
		u

#	Article	IF	CITATIONS
91	Study on the SPR responses of various DNA probe concentrations by parallel scan spectral SPR imaging. , 2008, , .		2
92	SPR sensor based on phase modulation and polarization interferometry. , 2006, , .		0